Computers & Geosciences 36 (2010) 16–23

Contents lists available at ScienceDirect

Computers & Geosciences

journal homepage: www.elsevier.com/locate/cageo

A MATLAB program for 1D strain rate inversion ☆

Hai-Bin Song [a,*], Lin Chen [a,b], Jiong Zhang [c], Chang-Yu Zhao [c], Chong-Zhi Dong [a,b]

[a] Key Laboratory of Petroleum Resources Research, Institute of Geology and Geophysics, Chinese Academy of Sciences, Beijing 100029, China
[b] Graduate University of Chinese Academy of Sciences, Beijing 100049, China
[c] School of Geophysics & Information Technology, China University of Geosciences, Beijing 100083, China

ARTICLE INFO

Article history:
Received 2 August 2008
Received in revised form
2 August 2009
Accepted 9 August 2009

Keywords:
Strain rate
Implicit finite difference scheme
Subsidence
MATLAB

ABSTRACT

This paper presents a MATLAB program designed to invert 1D strain rate from subsidence data. In forward modeling, we use an implicit finite difference scheme to solve the heat conduction equation with an advective term. In the inversion, we adopt the Powell algorithm to continually search for the optimal values of strain rate until the fit, defined by the difference between the calculated subsidence and the observed subsidence, is satisfactory. Synthetic datasets are generated, and one of them is used to test the inversion algorithm. The results show that the calculated subsidence fit the theoretical subsidence quite well, and the inverted strain rate oscillates around the true value and is a good approximation to the original strain rate variation. The program is applied to the northern continental margin of the South China Sea, and the inverted strain rate from WC1411 well reveals the multiple rifting events that occurred in this region. The inverted strain rate can be used to evaluate the stretching factor and provides constraints for dynamic modeling of lithospheric deformation.

1. Introduction

Over the past 30 years, there has been considerable interest in the evolution of rifts and passive continental margins. Tectonically active rifts, palaeo-rifts and passive margins form an important group of genetically related extensional basins among different types of sedimentary basin (Bally and Snelson, 1980). Extensional basins cover large areas of the globe and contain important mineral deposits and energy resources. A large number of major hydrocarbon provinces are associated with rifts and passive margins (White et al., 2003; Ziegler and Cloetingh, 2004). In order to understand the evolution of rifted basins, several models have been developed (McKenzie, 1978; Royden and Keen, 1980; Hellinger and Sclater, 1983; Rowley and Sahagian, 1986). When modeling subsidence, extension is usually assumed to be instantaneous (McKenzie, 1978) or to occur at a constant rate for a finite period of time (Jarvis and McKenzie, 1980). White (1993, 1994) has developed a method for inverting subsidence data, which has now been applied to many different basins (Newman and White, 1999; Xie et al., 2006).

In this paper, we present a study that aims to improve important aspects of the existing models and provides a useful tool for researchers studying the evolution of rifted basins. The purpose of this work is to provide an open MATLAB code suitable for inverting strain rate from subsidence data and evaluating stretching factor.

2. Physical model

We consider the 2D physical model shown in Fig. 1 (see Jarvis and McKenzie (1980) for further details). Crust and lithospheric mantle are stretched at horizontal velocity $u(x)$, and, at the same time, asthenospheric mantle flows upwards across the plane $z=0$ to replace the outflowing lithosphere. The upper surface, $z=a$, where a is the thickness of the lithosphere, is maintained at $T=0\,^{\circ}\mathrm{C}$ and the surface $z=0$ is maintained at $T=T_1$, the asthenospheric temperature. This form of boundary condition is clearly an approximation because the top of the lithosphere must subside and sediment should be deposited as stretching continues. Deformation is constrained to occur by pure shear strain, and the vertical velocity at $z=0$ is $G(t)a$, where $G(t)$ is the vertical strain rate as a function of time, t. The vertical velocity is required to vanish at $z=a$ and is therefore given by

$$v(z,t) = (a-z)G(t) \tag{1}$$

The time-varying temperature structure of the lithosphere is obtained by solving the 1D heat flow equation with an additional advective term

$$\frac{\partial T}{\partial t} + G(t)(a-z)\frac{\partial T}{\partial z} = \kappa\frac{\partial^2 T}{\partial z^2} \tag{2}$$

☆ Code available from server at http://www.iamg.org/CGEditor/index.htm.

* Corresponding author. Tel./fax: +86 10 82998142.
E-mail address: hbsong@mail.iggcas.ac.cn (H.B. Song).

0098-3004/$ - see front matter © 2009 Elsevier Ltd. All rights reserved.
doi:10.1016/j.cageo.2009.08.002

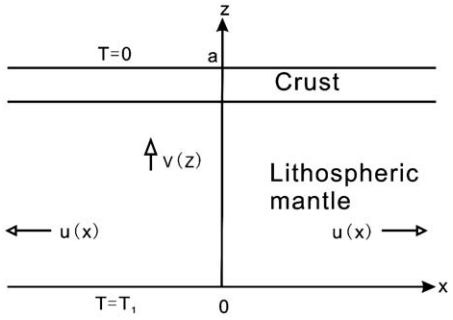

Fig. 1. Schematic diagram illustrating the physical model of time-dependent stretching of lithosphere. a=thickness of lithosphere; T_1=temperature of asthenosphere; $u(x)$=horizontal velocity and $v(z)$=vertical velocity.

where T is temperature, t is time, and κ is the thermal diffusivity. Conservation of material requires that

$$u(x,t) = xG(t) \tag{3}$$

Strain rate is not involved in the uniform stretching model, because it is assumed that stretching happens instantaneously in that model. In the finite stretching model (Jarvis and McKenzie, 1980), it is assumed that strain rate remains constant during lithosphere stretching (Wooler et al., 1992). In fact, strain rates vary with time.

Theoretical subsidence curves are normally generated as a function of β, the stretching factor (i.e. the total strain). These curves are fitted to the observed subsidence in order to determine β, which is related to vertical strain rate, $G(t)$, by

$$\beta = \exp\left(\int_0^{\Delta} G(t)dt\right) \tag{4}$$

where Δt is the duration of stretching.

If $G(t)$ is constant, then evaluating the integral yields

$$\beta = \exp(G\Delta t) \tag{5}$$

The standard expression for theoretical water-loaded subsidence (White, 1994) is

$$S(t) = A\left(1 - \frac{1}{\beta}\right) - BQ(t) \tag{6}$$

where

$$A = t_c(\rho_m - \rho_c)/(\rho_a - \rho_w) \tag{7}$$

$$B = \alpha\rho_m/(\rho_a - \rho_w) \tag{8}$$

$$Q(t) = \int_0^a [T(z,t) - T(z,\infty)]\, dz \tag{9}$$

$T(z,t)$ is the temperature of the lithosphere as a function of depth and time and $T(z,\infty)$ is the equilibrium temperature structure of the lithosphere. The symbols and values for other parameters are given in Table 1 (White, 1994). $Q(t)$ is a measure of the difference between the perturbed and equilibrium temperature structure and is a function of $G(t)$. A and B are crustal and lithospheric-mantle thinning factors, respectively.

The determination of subsidence as a function of time from knowledge of strain rate variation is defined as the *forward problem*.

The *inverse problem* can be solved directly by rearranging Eq. (6) (White, 1994)

$$G(t) = (d/dt)\left[\ln\left(\frac{A}{A - S(t) - BQ(t)}\right)\right] \tag{10}$$

Given $S(t)$, Eq. (10) can be solved iteratively to yield $G(t)$, using a starting distribution of $G(t)$ obtained by assuming $BQ(t)$=0, which means that the variation in density with temperature is initially ignored. $Q(t)$ is recalculated with the finite difference method in all subsequent iterations.

Table 1
Definition of parameters common to all calculations.

Symbol	Meaning	Value
a	Lithosphere thickness	125 km
t_c	Crustal thickness	30 km
ρ_w	Sea-water density	1.03 g/cm^3
ρ_c	Crust density (at 0 °C)	2.8 g/cm^3
ρ_m	Mantle density (at 0 °C)	3.33 g/cm^3
ρ_a	Asthenosphere density (at 1333 °C)	3.2 g/cm^3
α	Thermal expansion coefficient	3.28×10^{-5} °C^{-1}
Δt	Duration of stretching	40 Ma
β	Uniform stretching factor	
T	Temperature	
G	Strain rate	

Direct inversion necessitates numerical differentiation and is therefore susceptible to noise. For discrete and noisy data, the inverse problem is best solved by calculating a large number of forward models, varying only $G(t)$ each time until the difference between the calculated and the observed subsidences is minimized. We use Powell's algorithm (Press et al., 1992) to vary $G(t)$ systematically to minimize a trial function H (White, 1994)

$$H = \left[\frac{1}{N}\sum_{i=1}^{N}\left(\frac{S_i^o - S_i^c}{\sigma_i}\right)^2\right]^{1/2} + W_1\left[\frac{1}{M-1}\sum_{k=2}^{M}\left(\frac{G_k - G_{k-1}}{\delta t}\right)^2\right]^{1/2} + W_2\left[\frac{1}{M}\sum_{k=1}^{M}(G_k'')^2\right]^{1/2} + W_3\left[\frac{1}{M}\sum_{k=1}^{M}|\log(G_k)|\right] \tag{11}$$

where S_i^o and S_i^c are the observed and calculated subsidences, respectively; N is the number of observations of subsidence; M is the number of discrete values of $G(t)$; W_1, W_2, and W_3 are weighting coefficients and G''_k is estimates of the second derivative of $G(t)$ generated by cubic spline interpolation. The first term on the right-hand side of Eq. (11) is 0 when calculated and observed subsidences agree for all values. Dividing the difference between them by σ_i causes each term in the summation to have unit variance. The last three terms in Eq. (11) are added to attenuate the oscillation of inverted the results. The second and third terms cause $G(t)$ to be smooth, and the fourth term tends to infinity smoothly as any G_k approaches 0. We found that reasonable results are obtained when the weighting coefficients are set to W_1=0.5, W_2=0.5 and W_3=0.05.

3. Numerical model

The procedure used by Jarvis and McKenzie (1980) to solve Eq. (2) is a pseudo-analytic method, which involves the technique of separation of variables, eigenfunction expansion and numerical integration method such as the fourth-order Runge–Kutta method. Although Jarvis et al. (1980) intended to solved Eq. (2) analytically, their solution is based on numerical methods. Since it is difficult to find an analytic solution to Eq. (2), we adopt the finite difference method for solving Eq. (2). Using Crank–Nicolson implicit finite difference scheme (Lu and Guan, 2004), Eq. (2) can be written as

$$\frac{T_j^{n+1} - T_j^n}{\tau} + \frac{G(n\tau)(a - jh)}{2}\left(\frac{T_{j+1}^n - T_{j-1}^n}{2h} + \frac{T_{j+1}^{n+1} - T_{j-1}^{n+1}}{2h}\right)$$

$$= \frac{\kappa}{2}\left(\frac{T_{j+1}^{n} - 2T_{j}^{n} + T_{j-1}^{n}}{h^2} + \frac{T_{j+1}^{n+1} - 2T_{j}^{n+1} + T_{j-1}^{n+1}}{h^2}\right) \quad (12)$$

where τ and h are the temporal and spatial steps, respectively.

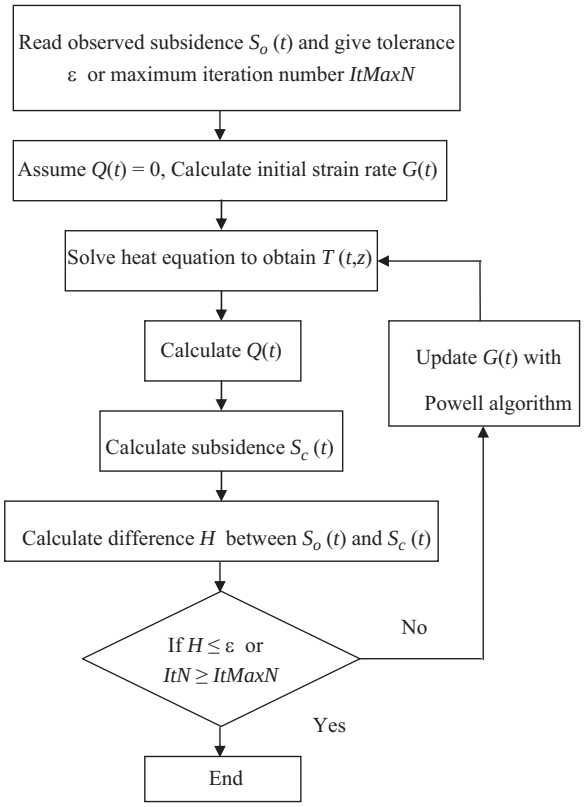

Fig. 2. Flowchart for inverting strain rate from subsidence data.

Let $\lambda = \kappa(\tau/h^2)$ and $r = (\tau/h)$, then Eq. (12) can be written as

$$\left[-\lambda - \frac{r}{2}G(n\tau)(a-jh)\right]T_{j-1}^{n+1} + 2(1+\lambda)T_{j}^{n+1} + \left[-\lambda + \frac{r}{2}G(n\tau)(a-jh)\right]$$

$$T_{j+1}^{n+1} = \left[\lambda + \frac{r}{2}G(n\tau)(a-jh)\right]T_{j-1}^{n} + 2(1+\lambda)T_{j}^{n} + \left[\lambda - \frac{r}{2}G(n\tau)(a-jh)\right]T_{j+1}^{n} \quad (13)$$

Given the initial temperature structure

$$T(z) = T_1(1 - z/a) \quad (14)$$

and boundary condition

$$T(t,a) = 0 \qquad T(t,0) = T_1 \quad (15)$$

Eq. (13) can be solved with the Thomas's algebraic scheme (Press et al., 1992).

For forward modeling, $G(t)$ is given. Therefore, once $T(t, z)$ is obtained, we can calculate subsidence with Eq. (6) and stretching factor with Eq. (4).

Given observed subsidence and guessed initial strain rate, $g_0(t)$ (i.e. let $Q(t)$ equal to zero and use Eq. (10) to determine $g_0(t)$), the inversion involves calculating a large number of forward models, varying only $G(t)$ each time until the difference between the calculated and the observed subsidences is minimized. The inverse flow is shown in Fig. 2.

4. Synthetic data

The algorithm described above has been applied to a set of synthetic data generated by forward modeling. The following equation was used to generate a strain rate distribution that decreased exponentially with time (White, 1994)

$$G(t) = G_0 \exp(-t/\tau) \quad (16)$$

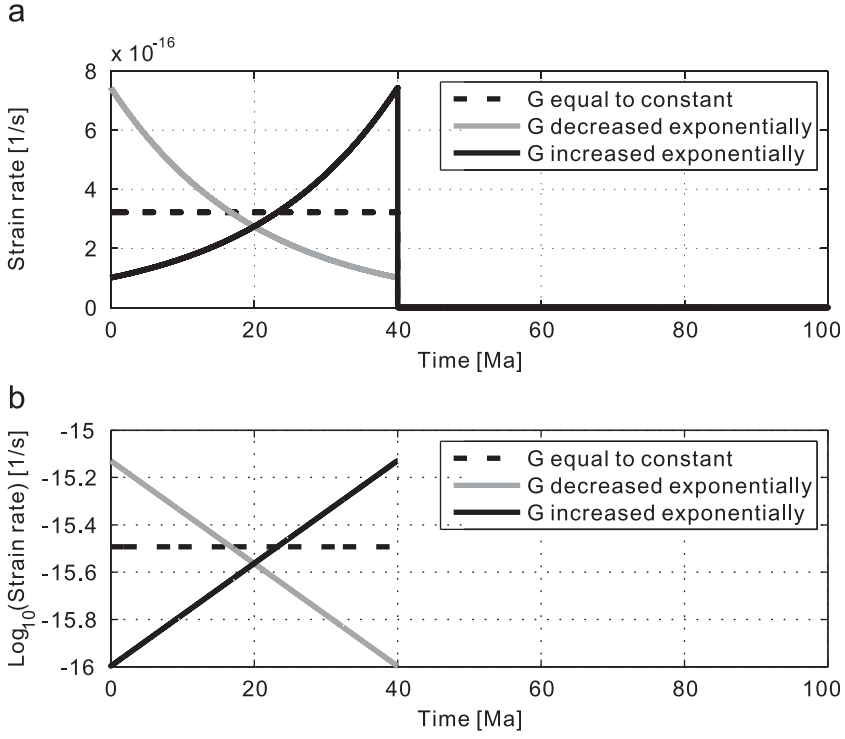

Fig. 3. Three strain rate profiles, all of which start at 0 Ma and end at 40 Ma, thus defining same rifting duration. In all three cases, the durations of stretching and total strain are identical. (a) Distribution of strain rate is displayed in true value and (b) profiles of strain rate are shown in logarithm.

where τ governs how quickly $G(t)$ decreases with increase in time and G_0 is a constant. G_0 is determined by

$$G_0 = \frac{\ln \beta}{\tau[1 - \exp(-\Delta t/\tau)]} \tag{17}$$

where Δt is the duration of stretching and β is the stretching factor.

Similarly, if $G(t)$ increases exponentially with time, then

$$G(t) = G_0 \exp(t/\tau) \tag{18}$$

$$G_0 = \frac{\ln \beta}{\tau[\exp(\Delta t/\tau) - 1]} \tag{19}$$

The forward modeling results of strain rate distributions shown in Fig. 3, 4 and 5 illustrate the effect that variations in $G(t)$ have on both subsidence and heat flow, given the total strain, β, is constant. We can see that if $G(t)$ is constant during the rift period, then the time derivatives of both the subsidence and the heat flow are approximately constant for the duration of rifting. When rifting ceases (i.e. G=0), subsidence and heat flow decay exponentially with time. In the second example, $G(t)$ decreases

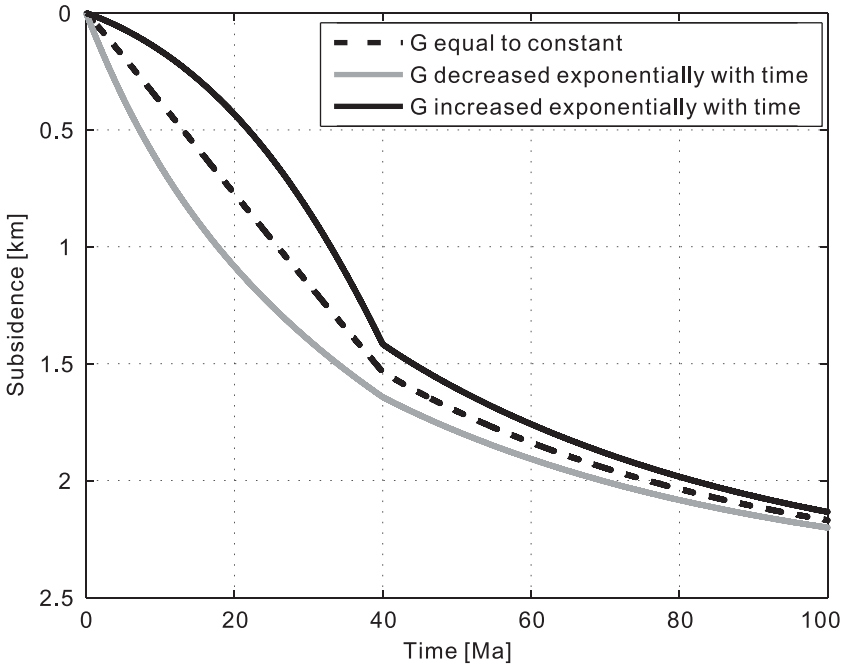

Fig. 4. Subsidence curves corresponding to strain rate distributions in Fig. 2.

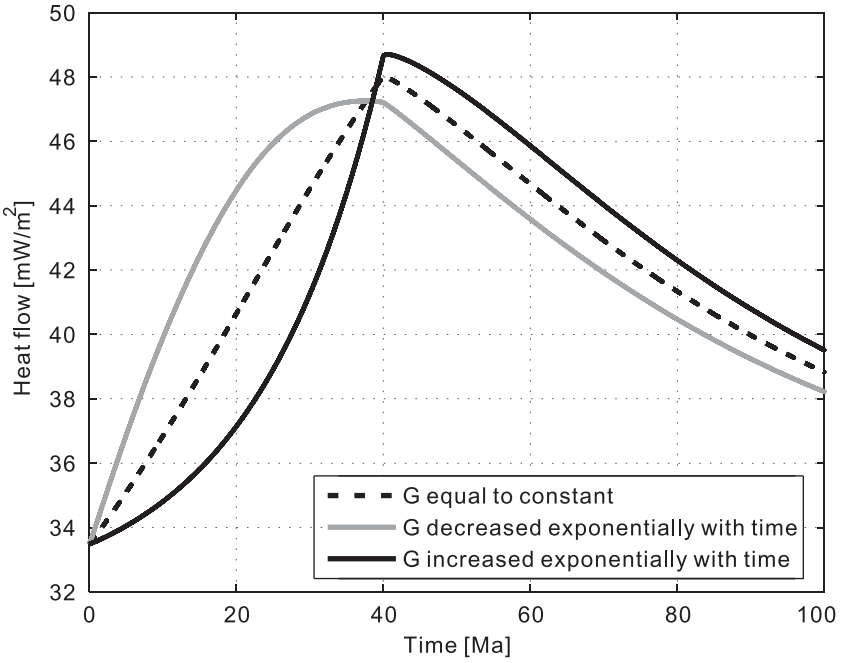

Fig. 5. Surface heat flow variation corresponding to strain rate distributions in Fig. 2.

exponentially with time and the syn-rift subsidence gradient also decreases with time. However, at the end of the rift period, subsidence must be greater than it is for constant $G(t)$ if the total strain is fixed. Finally, if $G(t)$ increases with time, the syn-rift subsidence gradient also increases with time but the total syn-rift subsidence is smaller than in the previous two examples. The heat flow shown in Fig. 5 has similar results as subsidence. The difference in the subsidence and heat flow curves is a consequence of the different distribution of strain rate during rifting. Once the disturbed temperature has returned to equilibrium, the total subsidence rates in all three cases are identical.

The inversion algorithm described above has been applied to a synthetic dataset generated by forward modeling with $G(t)$ decreasing exponentially with time during the rifting period. As shown in Fig. 6, the inverted strain rate oscillates around the true value. The calculated subsidence fits quite well with the theoretical subsidence except at the boundary and interrupted points, as shown in Fig. 7, where the standard deviations are set to 25 m for all observed data points. Although there are minor oscillations around the true values, the predicted subsidence fits the observed subsidence quite well. If the duration of rifting is known, then the inverted strain rate can be used to evaluate the stretching factor with Eq. (16). The calculated and theoretical stretching factor variations from the synthetic data are shown in Fig. 8. The results indicate that the variation of the stretching factor during the rifting is time-dependent.

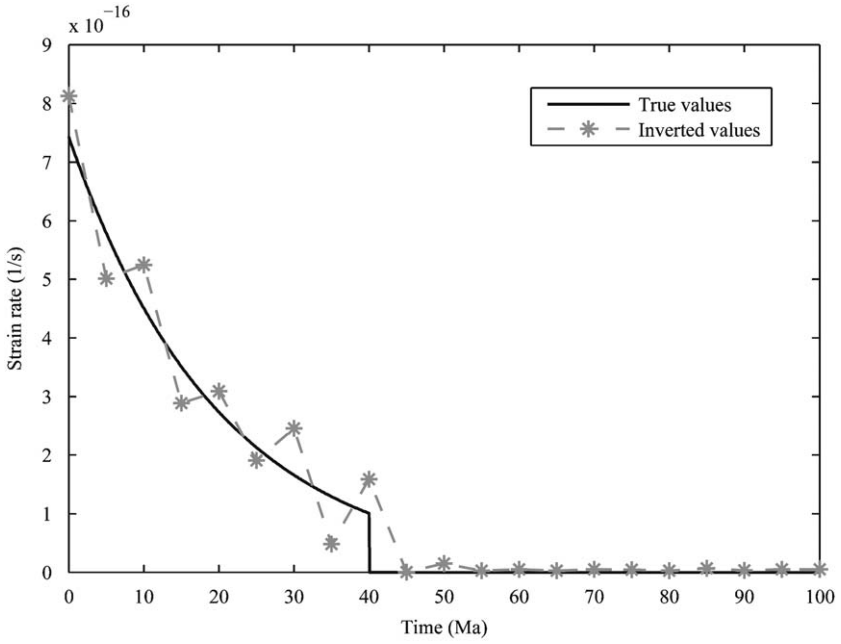

Fig. 6. Inverted strain rate for exponentially decreasing-type synthetic data.

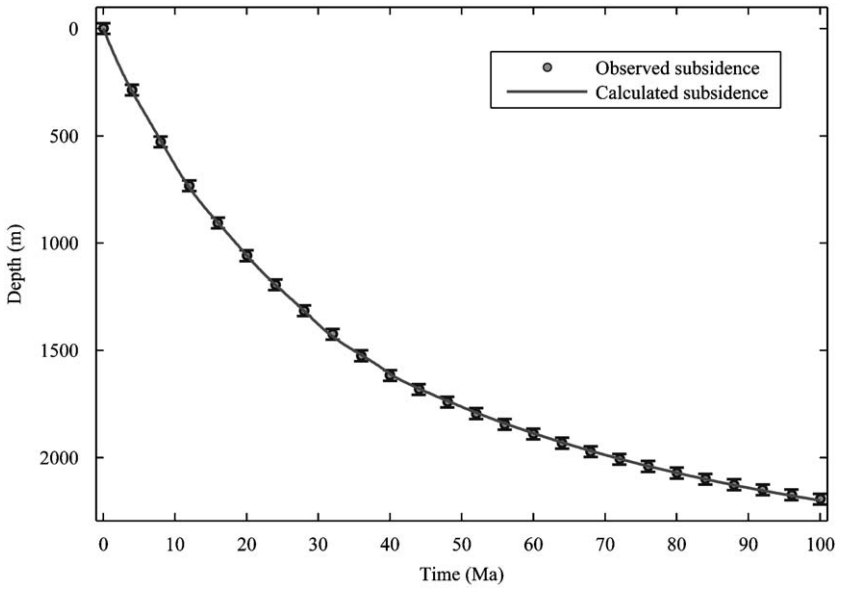

Fig. 7. Relation between observed and calculated subsidences.

5. Application to the South China Sea

The South China Sea (SCS) is one of the largest marginal seas in the western Pacific, which is located at the junction of the Eurasian plate, the Pacific Plate and the Indian–Australian plate. It was formed by continent breakup and sea-floor spreading in the Cenozoic (Taylor and Hayes, 1980; Briais et al., 1993). The northern continental margin of the SCS experienced multiple rifting events

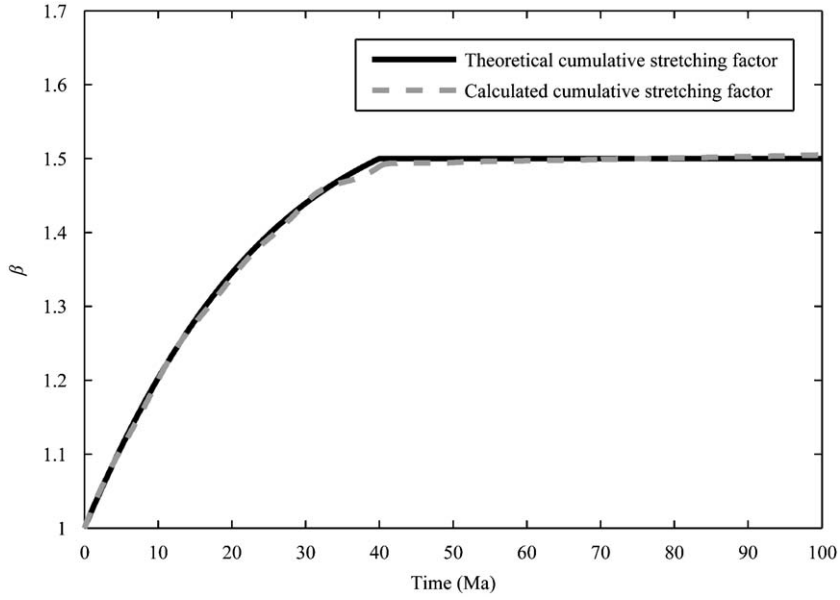

Fig. 8. Calculated and theoretical cumulative stretching factor variation computed with inverted and true strain rates, respectively.

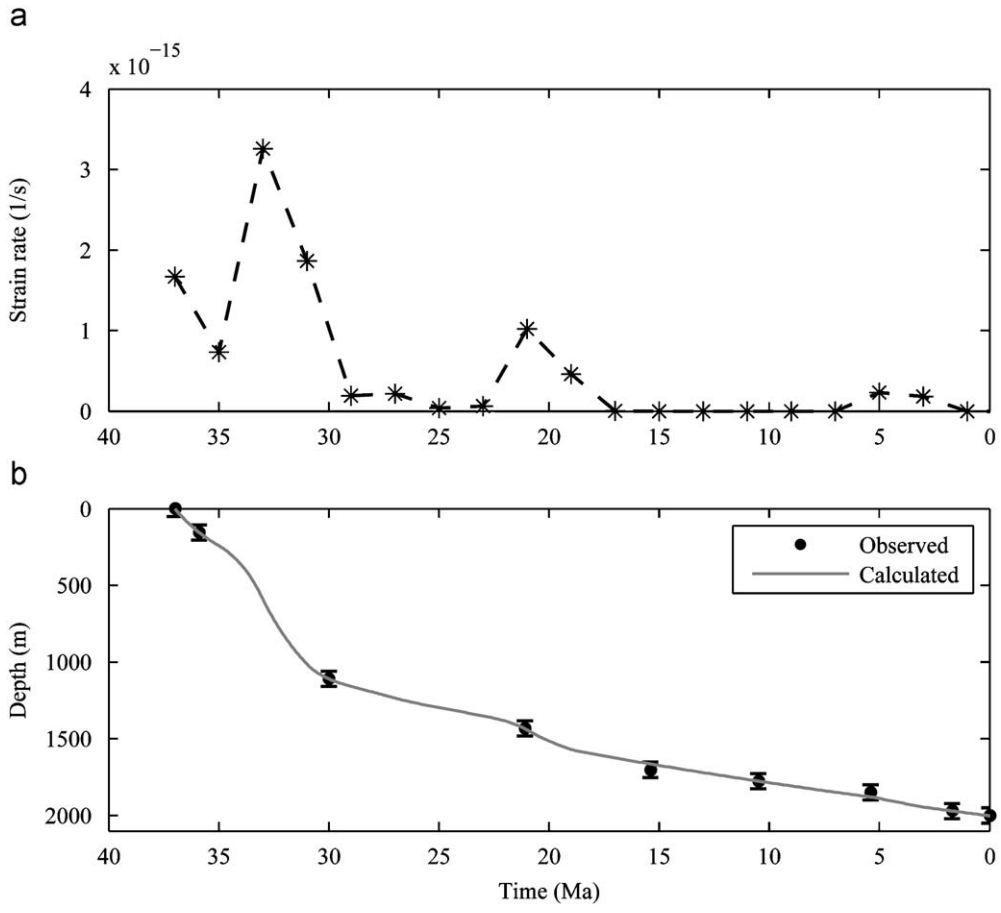

Fig. 9. Inverted strain rate of WC1411 well. (a) Inverted strain rate distribution of WC1411 well and (b) observed subsidence (black solid points) and predicted subsidence (gray solid line).

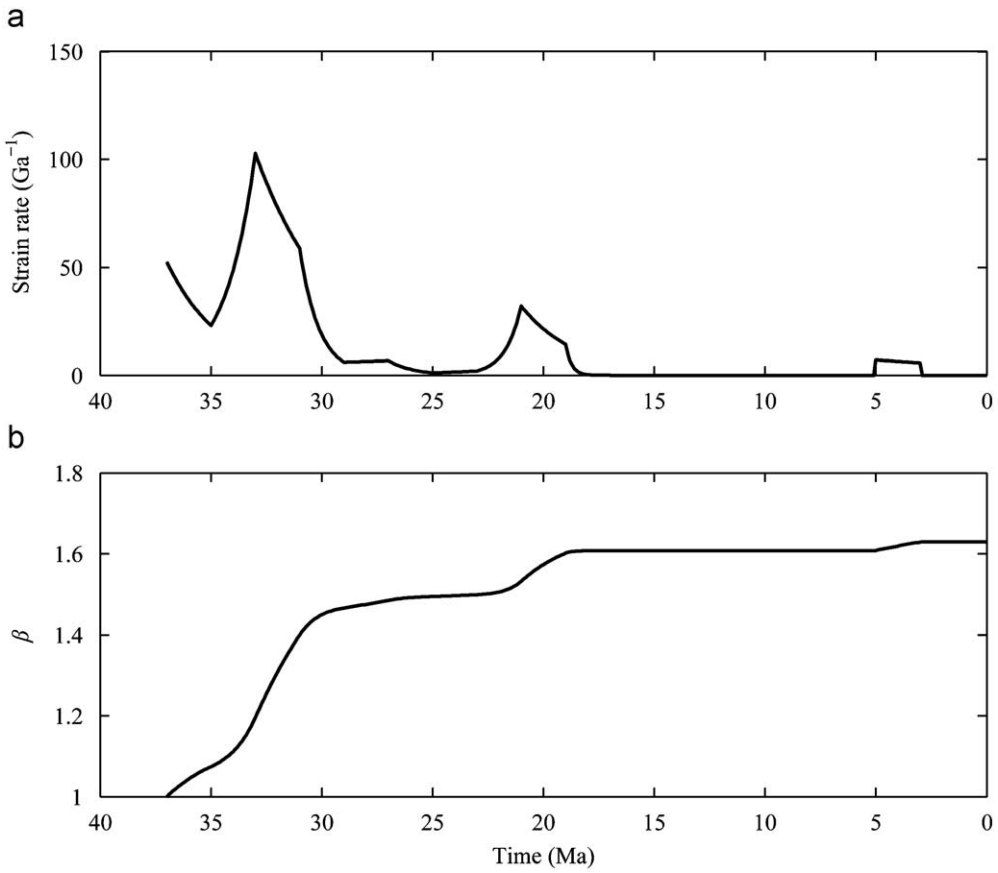

Fig. 10. Stretching factor estimated from strain rate of WC1411 well. (a) Distribution of strain rate of WC1411 well and (b) accumulative stretching factor of WC1411 derived from integral of strain rate.

(Ru and Pigott, 1986; Clift and Lin, 2001; He et al., 2002). We apply our Matlab program to invert strain rate and estimate stretching factor of the northern continental margin of the SCS with tectonic subsidence data from a drilling well. The data is derived from Xie et al. (2006).

Fig. 9 shows the inverted strain rate of WC1411 well, which is located at the Pearl River Mouth Basin (PRMB) in the northern continental margin of the SCS. The subsidence data is derived from Xie et al. (2006). The standard deviation is assumed to be 25 m for all the observed data. Fig. 10 shows the accumulative stretching factor of the WC1411 well, which is the exponent of the integral of the strain rate. The strain rate distribution shown in Fig. 9(a) reveals the multiple rifting events in this region. The strain rate can help us understand the rifting process. During the inversion of the strain rate of the WC1411 well, the crustal and lithospheric thicknesses are set to 30 and 120 km, respectively according to Yao et al. (1994), and other used parameters are the same as Table 1.

6. Conclusions

A MATLAB program is designed to invert strain rate variation as a function of time by fitting observed subsidence curve from extensional sedimentary basins. As White (1994) pointed out, this method does not require prior information concerning either the duration of rifting or the total strain. A set of synthetic data is generated to test this method. The calculated subsidence fits the observed (or theoretical) subsidence quite well. Although the inverted strain rate oscillates around the true value, the inverted result reflects the original trend of the strain rate variation. Furthermore, the inverted strain rate can be used to evaluate stretching factor. The resultant information concerning the temporal strain rate variation provides constraints required for the dynamic modeling of lithospheric deformation. Strain rate does not only vary temporally but also spatially. Recently, White and Bellingham (2002) generalize 1D strain rate inversion to 2D case, and Shillington et al. (2008) describe a similar algorithm which inverts 2D depth-dependent strain rate. In order to deal with real-world problems, future development will involve implementing a 2D strain rate inversion program based on this program and White's recent work.

Acknowledgements

This study is supported by the National Major Fundamental Research and Development Project of China (No. 2007CB411704) and by the Marine Facies Foresight Project of the China Petroleum and Chemical Corporation. We appreciate the comments of Dr. N. White and an anonymous reviewer. We would like to thank Dr. Vincent Tong of University of London for polishing English for our paper.

References

Bally, A.W., Snelson, S., 1980. Realms of subsidence. In: Miall, A.D. (Ed.), Facts and Principles of World Petroleum Occurrence. Canadian Society of Petroleum Geologists, Memoir 6, pp. 9–94.

Briais, A., Patriat, P., Tapponnier, P., 1993. Updated interpretation of magnetic anomlies and seafloor spreading stages in the South China Sea: implication for the tertiary tectonics of Southeast Asia. Journal of Geophysical Research 98, 6299–6328.

Clift, P., Lin, J., 2001. Preferential mantle lithospheric extension under the South China margin. Marine and Petroleum Geology 18, 929–945.

He, L.J., Xiong, L.P., Wang, J.Y., 2002. Heat flow and thermal modeling of the Yinggehai Basin, South China Sea. Tectonophysics 351, 245–253.

Hellinger, S.J., Sclater, J.G., 1983. Some comments on two-layer extensional models for the evolution of sedimentary basins. Journal of Geophysical Research 88, 8251–8270.

Jarvis, G.T., McKenzie, D., 1980. Sedimentary basin formation with finite extension rates. Earth and Planetary Sciences Letters 48, 42–52.

Lu, J.F., Guan, Z., 2004. Numerical Methods for Partial Differential Equations (in Chinese), second ed. Tsinghua University Press, Beijing, China 318pp.

McKenzie, D., 1978. Some remarks on the development of sedimentary basins. Earth and Planetary Sciences Letters 40, 25–32.

Newman, R., White, N., 1999. The dynamics of extensional sedimentary basins: constraints from subsidence inversion. Philosophical Transactions of the Royal Society of London 357 (1753), 805–834.

Press, W.H., Flannery, B.P., Teukolsky, S.A., Vetterling, W.T., 1992. Numerical recipes in C: The Art of Scientific Computing, second ed. Cambridge University Press, London 994pp.

Rowley, D.B., Sahagian, D., 1986. Depth-dependent stretching: a different approach. Geology 14, 32–35.

Royden, L., Keen, C.E., 1980. Rifting processes and their evolution of the continental margin of eastern Canada determined from subsidence curves. Earth and Planetary Sciences Letters 51, 343–361.

Ru, K., Pigott, J.D., 1986. Episodic rifting and subsidence in the South China Sea. AAPG (American Association of Petroleum Geologists). Bulletin 70, 1136–1155.

Shillington, D.J., White, N., Minshull, T.A., 2008. Cenozoic evolution of the eastern Black Sea: a test of depth-dependent stretching models. Earth and Planetary Sciences Letters 265, 360–378.

Taylor, B., Hayes, D.E., 1980. The tectonic evolution of the South China Sea. In: Hayes, D.E. (Ed.), Tectonic and Geological Evolution of Southeast Asia Seas and Islands. American Geophysical Union, Monograph 23, pp. 89–104.

White, N., 1993. Recovery of strain rate variation from inversion of subsidence data. Nature 366, 499–552.

White, N., 1994. An inverse method for determining lithosperic strain rate variation on geological timescales. Earth and Planetary Sciences Letters 122, 351–371.

White, N., Bellingham, P., 2002. A two-dimensional inverse model for extensional sedimentary basins 1. Theory. Journal of Geophysical Research 107 (B10), 2259, doi:10.1029/2001JB000173.

White, N., Thompson, M., Barwise, T., 2003. Understanding the thermal evolution of deep-water continental margins. Nature 426, 334–343.

Wooler, D.A., Smith, A.G., White, N., 1992. Measuring lithospheric stretching on Tethyan passive margins. Journal of the Geological Society 149, 517–532.

Xie, X., Müller, R., Li, S., Gong, Z., Steinberger, B., 2006. Origin of anomalous subsidence along the Northern South China Sea margin and its relationship to dynamic topography. Marine and Petroleum Geology 23, 745–765.

Yao, B.C., Zeng, W.J., Hayes, D.E., Spanger, S., 1994. The Geological Memoir of South China Sea Surveyed Jointly by China and USA (in Chinese). China University of Geosciences Press, Wuhan, China 102 pp.

Ziegler, P.A., Cloetingh, S., 2004. Dynamic process controlling evolution of rifted basins. Earth-Science Reviews 64, 1–50.